

AN ASYMPTOTIC FORMULATION FOR THE INFUSION OF A THERAPEUTIC AGENT INTO A SOLID TUMOR MODELED AS A POROELASTIC MEDIUM

Alessandro Bottaro and Tobias Ansaldo
DICAT – Centro di Ricerca in Tecnologie dei Materiali
Università di Genova
1, via Montallegro, 16145 Genova, Italy

Abstract

The direct infusion of an agent into a solid tumor, modeled as a spherical poroelastic material with anisotropic dependence of the tumor hydraulic conductivity upon the tissue deformation, is treated both by solving the coupled fluid/elastic equations, and by expressing the solution as an asymptotic expansion in terms of a small parameter, ratio between the driving pressure force in the fluid system and the elastic properties of the solid. Results at order one match almost perfectly the solutions of the full system over a large range of infusion pressures. A comparison with experimental results by McGuire et al. (2006) provides acceptable agreement after the hydraulic conductivity of the medium is properly calibrated. Given the wide range of variation of some model constants, the order zero solution of the expansion – for which fluid and porous matrix are decoupled – yields acceptable values and trends for all the physical fields of interest. When the deformation of the tissue becomes large nonlinear elasticity theory must be resorted to.

1. Introduction

In recent years it has become common to shrink solid tumors before surgery via intratumoral injection of chemotherapeutic drugs, to allow cleaner/simpler/less destructive removal, or to render operable possibly inoperable tumors. Efficient delivery of a therapeutic agent within a solid tumor via intratumoral infusion requires a thorough understanding of the fluid dynamics in the gel-like region between cells (the *interstitium*). A number of physiological barriers opposes the infusion: the abnormally elevated density of cancer cells limits drug transport by constricting intratumoral blood vessels; the high interstitial fluid pressure (IFP) which occurs within the tumor and the lack of functional lymphatics hamper convective transport of the agents to the interstitium; and the tumor microvasculature is leaky. The main obstacle to efficient delivery is believed to be the high IFP (values up to 50 mmHg have been reported in solid tumors, Baxter and Jain 1989; Boucher et al. 1991; Roh et al. 1991; Gutmann et al. 1992); it can produce some reabsorption of fluid by the capillary network with the consequence that not all the therapeutic agent injected diffuses within the tumor tissues.

It is common to model the problem of the transport of drugs and nutrients within a solid tumor by considering it as a fluid-saturated porous medium, characterized by the hydraulic conductivity K of the tissue (ratio between the permeability of the medium and the dynamic viscosity of the fluid) and by its Lamé coefficients, G and λ . Assuming negligible lymphatic drainage, the parameters needed to describe transvascular fluid exchange – within the Starling's law assumption – are the

hydraulic conductivity of the capillary walls L_p , the vascular surface area per unit volume S/V and the effective vascular pressure p_e . Macroscopic parameters can in principle be inferred from homogenizing the microscopic features of the tumor, i.e. its morphology as a micro-structured material, with fiber matrix, proteins, fluid in the interstitial matrix, and including the fluid exchange with the capillaries embedded in the interstitium (see Shipley and Chapman (2010) for recent progress on this). A more common approach is to infer values of the governing parameters from *in vivo* and *in vitro* measurements. Smith and Humphrey (2007) provide a review of measured values from the literature.

The rate of fluid flow within the tumor depends on the value of K of the tissues which can, in turn, be strongly altered by the deformation of the tissues themselves. It has been found (Zhang et al. 2000) that variations of the hydraulic conductivity by several orders of magnitude may take place with a four-fold increase of the infusion pressure, as a result of tissue expansion and compression. The coupling between the deformation of the tumor and its conductivity is hence crucial, and the use of poroelasticity theory has been proposed, see for example Netti et al. (1995) or Sarntinoranont et al. (2003). Whereas various empirical relations for $K = K(u)$, with u the displacement of the solid, are present in the literature (ex. Lai and Mow 1980; Barry and Aldis 1990), only McGuire et al. (2006) consider a non-linear, anisotropic relation.

In this work we follow the lead of McGuire et al. (2006) to study the intratumoral infusion of a therapeutic agent into an isolated solid tumor of spherical shape, i.e. a tumor that is not surrounded by normal tissue. A perturbation approach is proposed within the linear elastic approximation, with the solution expressed in term of powers of a small dimensionless parameter δ , defined as the ratio between an effective pressure at the infusion site and the tissue solid properties (expressed via a linear combination of G and λ). Comparison between results obtained with the full model and with the perturbation analysis (up to order δ) provide an indication on the range of applicability of the asymptotic approach.

2. The model

Tumors are strongly heterogeneous and are often modeled as being formed by concentric layers of tissue (eventually including a necrotic core) of thickness defined by the proliferation/quiescent activity of the cancer cells; here, we consider a spherical tumor of radius R , whose sources of radial inhomogeneity are in the hydraulic conductivity of the tumor interstitium K and in the hydraulic conductivity of the capillary walls L_p . A drug is infused at the center by a needle, creating a small fluid cavity around the tip of radius a (cf. fig. 1). As fluid is injected, the cavity deforms mildly and, at the steady state, the fluid fills a spherical cavity of radius a' . Likewise, the radius of the tumor becomes R' in steady infusion conditions. Spherical symmetry is maintained and the radial component σ_{rr} of the stress tensor \mathbf{T} , in the linear elastic approximation, is

$$\sigma_{rr} = -p + (2G + \lambda) u_r + 2\lambda u/r \quad (1)$$

with p the IFP, u the radial displacement of the solid, and r the radial coordinate (when r is used as subscript a derivation is intended, except when the subscript denotes the component of a tensor, ex. σ_{rr} or ε_{rr}). The term $[(2G + \lambda) u_r + 2\lambda u/r]$ is the radial contact stress. By setting to zero the divergence of \mathbf{T} it is obtained:

$$(2G + \lambda)(u_r + 2u/r)_r = p_r \quad (2)$$

The conservation of mass in the fluid phase within the Darcy flow assumption is:

$$-(r^2 K p_r)/r^2 = L_p (p_e - p) S/V \quad (3)$$

with the right-hand-side, the Starling's law term, which can act as either a source or a sink because of the leakiness of the tumor microvasculature. Since the tumor vasculature is structurally and functionally abnormal, it is common to assume a constant value of p_e ; conversely, to account for the heterogeneous distribution of capillaries, and in particular for the increased activity of cancer cells towards the outer boundary of the tumor, where they coopt host vessels to obtain nutrients for their growth and sprout new vessels from existing ones, we assume L_p to vary with r as:

$$L_p = L_{p0} f(r/R), \quad (4)$$

with $f(r/R)$ a dimensionless function ranging from zero to one

To model anisotropic effects in the hydraulic conductivity K we assume, following McGuire et al., that

$$K = K_0 \exp\{M[\alpha \varepsilon_{rr} + (1 - \alpha) (\varepsilon_{\theta\theta} + \varepsilon_{\phi\phi})/2]\} \quad (5)$$

with K_0 , M , α model constants, ε_{rr} , $\varepsilon_{\theta\theta}$ and $\varepsilon_{\phi\phi}$ components of the strain tensor defined by $\varepsilon_{rr} = u_r$ and $\varepsilon_{\theta\theta} = \varepsilon_{\phi\phi} = u/r$. The equations are closed by boundary conditions, i.e.

$$\begin{aligned} p(R') &= 0; \quad p(a') = p_{\text{infusion}}; \quad (2G + \lambda) u_r(R') + 2\lambda u(R')/R' = 0; \\ -p(a') + (2G + \lambda) u_r(a') + 2\lambda u(a')/a' &= -p_{\text{infusion}}. \end{aligned} \quad (6)$$

The latter two relations specify, respectively, the absence of radial contact stresses at the tumor margins $r = R'$, and the continuity of the radial components of the stress across the interface in $r = a'$ between the cavity and the porous matrix (Truskey et al. 2009). Since a' and R' are a priori unknown, the boundary conditions in the full model are enforced at a and R , under the hypothesis of small deformations.

Normalization of equations and boundary conditions brings out the relevant parameters of this model. We thus scale the IFP with $(p_{\text{infusion}} - p_e)$, the displacement u and the radial coordinate r with R , and the hydraulic conductivity K with K_0 , isolating two dimensionless parameters:

$$\delta = (p_{\text{infusion}} - p_e)/(2G + \lambda) \quad (7)$$

$$\gamma^2 = (L_{p0}/K_0) R^2 S/V \quad (8)$$

The first parameter characterizes the ratio between the driving pressure forces in the fluid system and the elastic properties of the solid; the second parameter measures the relative importance of the resistance to interstitial percolation with respect to the resistance to transcapillary fluid exchange (Baxter and Jain 1989, 1990). Typically δ is much smaller than one, whereas γ is of order one.

The equations in terms of dimensionless variables read:

$$(u_r + 2u/r)_r = \delta p_r \quad (9)$$

$$(r^2 K p_r)_r = r^2 \gamma^2 (p - p_e) f(r) \quad (10)$$

$$K = \exp\{M[\alpha u_r + (1 - \alpha) u/r]\} \quad (11)$$

with boundary conditions:

$$p(1) = 0; p(a) = p_{\text{infusion}}; u_r(1) + 2\lambda/(2G + \lambda) u(1) = 0; u_r(a) + 2\lambda/(2G + \lambda) u(a)/a = 0 \quad (12)$$

and a now scaled by R . Equations (9-12) are solved by a finite difference second order iterative scheme, yielding solutions for p , the hydraulic conductivity K , the Darcy flux $q = -K p_r$ and the flow rate Q of the therapeutic agent through the tumor, for parameters corresponding to some of the measurements by McGuire et al. We denote with Q_{infusion} the value of Q at $r = a$.

3. The perturbation approach

A second approach to the solution of the problem begins by expanding the dependent variables into regular power series of δ (Bonfiglio et al. 2010) as:

$$u = \delta u_1 + O(\delta^2),$$

$$p = p_0 + \delta p_1 + O(\delta^2),$$

$$K = 1 + \delta K_1 + O(\delta^2),$$

with $K_1 = M[\alpha u_{1r} + (1 - \alpha) u_1/r]$. Upon inserting into equation (10) the equation at order 0 is:

$$(r^2 p_{0r})_r = r^2 \gamma^2 (p_0 - p_e) f(r), \quad (13)$$

with boundary conditions $p_0(1) = 0$ and $p_0(a) = p_{\text{infusion}}$. The solution in the $L_p = L_{p0}$ limit is simply:

$$p_0 = p_e + A e^{\gamma r}/r + B e^{-\gamma r}/r \quad (14)$$

with A and B easily available from the boundary conditions. For $f(r)$ not uniformly equal to one, the zeroth order pressure field can be found by numerical integration of eq. (13). From p_0 it is then easy to recover the leading order Darcy flux q_0 and flow rate Q_0 . At order δ the equations are:

$$(u_{1r} + 2u_1/r)_r = p_{0r} \quad (15)$$

$$(r^2 K_0 p_{1r} + r^2 K_1 p_{0r})_r = r^2 \gamma^2 p_1 f(r), \quad (16)$$

together with

$$p_1(1) = -u_1(1) p_{0r}(1)$$

$$p_1(a) = -u_1(a) p_{0r}(a)$$

$$u_{1r}(1) + 2\lambda/(2G + \lambda) u_1(1) = 0$$

$$u_{1r}(a) + 2\lambda/(2G + \lambda) u_1(a)/a = 0 \quad (17)$$

obtained by Taylor expanding the boundary conditions in eq. (6) around $r = a$ and $r = R$, and collecting terms of order δ . The variables p_1 , K_1 and u_1 , as well as q_1 and the infusion flow rate at order δ , can be obtained by a central difference numerical method, similar to that used for eqs. (9-12). In both cases we have employed a large number of uniformly distributed radial grid points (up to 6000) to ensure that all results presented are grid-converged.

4. Results

The configuration examined here correspond to the 4T1 cell lines used in the study by McGuire et al. These lines had the highest collagen concentration among the tested ones, and showed a strongly non-linear relation between the infusion pressure and the infusion rate. They were murine mammary carcinoma cell lines, injected subcutaneously into mice. After the tumor had grown to a diameter of the order of the centimeter, a solution was infused into the center of the tumor with a needle, until a small fluid cavity approximately equal to the needle radius was formed. From that point on, increasing and measuring the infusion pressure, McGuire et al. could measure the corresponding flow rate of the solution entering the tissue. Errors on the measured pressures could be quantified to be less than 3.7 mmHg. In table 1 a list of all parameters employed in the present simulations is given.

Physical variable or model constant	Definition	Corresponding dimensionless value
$a = 0.18$ mm	Unperturbed radius of the inner cavity	$a = 0.036$
$R = 0.5$ cm	Unperturbed radius of the tumor	$R = 1$
$K_0 = 3 \times 10^{-5}$ cm ² /(mmHg s) (smaller values are typically given in the literature, e.g. Smith and Humphrey 2007)	Model constant in eq. (5)	

$M = 10$	Model constant in eq. (5)	
$0 < \alpha < 1$; $\alpha = 0.733$ was the best fit with the data for the model by McGuire et al.	Model constant in eq. (5)	
$P_e = 11.25$ mmHg	Effective vascular pressure (Smith and Humphrey 2007)	
$30 \text{ mmHg} \leq p_{\text{infusion}} \leq 70 \text{ mmHg}$	Infusion pressure	$1.6 \geq p_{\text{infusion}} \geq 1.1915$
$L_{p0} = 1.3332 \times 10^{-6} \text{ cm}/(\text{mmHg s})$	Vascular conductivity at $r = R$ (Smith and Humphrey 2007)	
$S/V = 200 \text{ cm}^2/\text{cm}^3$	Vascular surface area per unit volume (Smith and Humphrey 2007)	$\gamma^2 = 2.2222$ (eq. 6)
$10 \text{ mmHg} \leq \lambda \leq 1000 \text{ mmHg}$; $\lambda = 175$ mmHg was the best fit with the data for the model by McGuire et al.	Lamé coefficient	
$G = 75$ mmHg (corresponding to $\lambda = 175$ mmHg once the Poisson ratio ν is fixed at 0.35)	Shear modulus	
$0.05769 \leq \delta \leq 0.1807$	Small parameter in the expansion (eq. 7)	

Table 1: List of relevant dimensional and dimensionless parameter. All of them have been taken from McGuire et al. except where otherwise indicated.

Three cases are considered next, denoted as cases 1, 2 and 3. The first assumes a constant value of $L_p = L_{p0}$, i.e. $f(r) = 1$. In the second case it is assumed that $f(r)$ increases radially outwards as $f(r) = \exp[b(r-1)/(1-a)]$, with $b = \log(10)$; the value of L_p at $r = R$ is equal to L_{p0} and it is ten times larger than the corresponding value at $r = a$. The factor of ten is arbitrary, but within the range of values reported in the literature (Baxter and Jain 1989; Smith and Humphrey 1997). In the third case we make the hypothesis that transvascular fluid exchange is concentrated near the tumor outer margins, possibly as a result of strong localized angiogenesis, so that $f(r) = \exp[-150(r-1)^2]$. These three distributions cover a large spectrum of configurations, and are plotted in fig. 2. In figs. 3 and 4 results are reported from simulations using the full model, i.e. eqs. (9-12), at $\delta = 0.05$ (corresponding to $p_{\text{infusion}} = 27.5$ mmHg) and $\delta = 0.2$ ($p_{\text{infusion}} = 76.25$ mmHg). As expected the deformation u is larger for larger infusion pressure. The trend of the u -curves with r varies with the case considered: it decreases rapidly near the infusion site for all cases, to eventually increase (case 1), settle (case 2) or slowly decrease (case 3). Perhaps unexpectedly the conductivity K of the tissue is but mildly affected by variations in the hydraulic conductivity of the capillary walls; in both fig. 3 and 4 one observes a very steep increase of K from the infusion point, and a rapid equilibration around $K \approx 1$. The IFP decreases monotonically in r from p_{infusion} to zero, with little effect of L_p , while the flow rate increases. This is related to extravasation of fluid from the vessels into the tumor interstitium, not balanced by resorption into lymphatics.

Denoting by Q_{infusion} the rate of agent entering the tumor at $r = a$, the (now dimensional) variation of Q_{infusion} with p_{infusion} is displayed in fig. 5, for the three cases of fig. 2. It is interesting to observe that for the value of K_0 employed by McGuire et al. – which is the average value measured in their experiments – our model overestimates the infusion rate. On the other hand, values of the average hydraulic conductivity typically lower than $3 \times 10^{-5} \text{ cm}^2/(\text{mmHg s})$ are often reported for neoplastic tissues (see e.g. Smith and Humphrey (2007) who report a range between $4 \times 10^{-9} \text{ cm}^2/(\text{mmHg s})$ and $2.5 \times 10^{-6} \text{ cm}^2/(\text{mmHg s})$). In fig. 5 we have therefore also included results for the three cases of figure 2 for a value of K_0 ten times smaller than indicated by McGuire et al., obtaining a better match with experimental data. McGuire et al. observed a marked reduction of the infusion rate after the infusion pressure exceeds 50 mmHg (cf. fig. 4, bottom frame, of McGuire et al.) and argued that the bell-shaped curve in the $p_{\text{infusion}}-Q_{\text{infusion}}$ plane is partly related to the formation of a thin membrane around the needle tip, forcing the pressure at $r = a$ to be above a given threshold before intratumoral infusion can take place. The existence of a threshold pressure for infusion had been observed previously (McGuire and Yuan 2001) and the mechanism still awaits a complete physical description. Another possible reason of discrepancy between the numerical results that we have obtained and those by McGuire et al. is due to the neglect/account of fluid exchange between the interstitium and the blood vessels. Accounting for it, via the Starling's law term, we find that Q increases with r with fluid filling the extra-cellular matrix and contributing to the increase of the strain. Fig. 5 shows also results obtained from the asymptotic model at order zero, with constant $L_p = L_{p0}$ (i.e. results directly available from eq. 14). It is interesting to observe that – particularly at low infusion pressures – they do not differ much from the solutions of the full system (9-12), and are similarly affected by variations in K_0 . As expected, the agreement between the exact solution of the full model and the leading order solution deteriorates with the increase of δ . Given the uncertainties in the estimate of the hydraulic conductivity, for practical purposes, in the limit of very small deformations, it seems that the leading order term of the expansion yields field values which are sufficiently accurate. On the other hand, for “large” deformations (within the limits of linear elasticity theory), it is appropriate to extend the asymptotic solution up to next higher order.

The accuracy of the expansion proposed can be inferred from inspection of figs. 6 and 7. Here the solutions, up to order δ , of the asymptotic model are drawn together with the results of the full system of equations (9-12), for two cases, $\delta = 0.1$ and 0.3 , corresponding, respectively, to $p_{\text{infusion}} = 43.75 \text{ mmHg}$ and $p_{\text{infusion}} = 108.75 \text{ mmHg}$. Case 1 has been treated in both figures. The agreement is generally good, despite the fact that the larger value of p_{infusion} exceeds by much those commonly encountered in applications; such a large value of δ is of interest only to test the limitations of the asymptotic analysis. The validity of the latter statement stems also from Jain's (1987) observation that the porosity ϕ of the interstitial matrix is approximately 0.2; this means that the pore velocity (equal to the Darcy flux q divided by ϕ) can be properly represented by the expansion proposed only when δ is much smaller than 0.2. In the results shown here we have fixed K_0 to the value of $3 \times 10^{-6} \text{ cm}^2/(\text{mmHg s})$ which appears to provide flow rates of the agent at $r = a$ closer to the measured ones. The plots of the IFP resemble those presented by Smith and Humphrey (2007) for a similar configuration. The pressure decays over a small radial distance

from the infusion site, it remains close to the effective vascular pressure over a range of r , before ultimately decaying to the value imposed at the tumor margin. When the infusion pressure is very large ($\delta = 0.3$) the agreement between the asymptotic solution at order δ and the full solution deteriorates, particularly as far as u is concerned, yielding a negative value of the hydraulic conductivity very close to the infusion site; whereas one could go to second order to improve matters, this is not consistent with linear elasticity theory which holds to first order in the deformation.

5. Closing remarks

An asymptotic approach has been proposed for the study of the infusion of a therapeutic agent into a solid tumor, modeled as a poroelastic medium of conductivity anisotropically dependent on the material strain rate. In the model we have included fluid exchange with the capillary, and observed the minor influence of variations of the vascular conductivity L_p on the results. The parameter which influences the most the results is the average hydraulic conductivity K_0 of the medium, whereas the radial distribution of K holds a relatively minor role. Given the large scatter of data present in the literature for K_0 , there seems to be little need in coupling the elastic deformation of the fluid with the hydraulic properties of the interstitium: the leading order, uncoupled, solution is sufficiently accurate, at least for sufficiently low values of the infusion pressure. The situation is obviously different should large strains of the tissue occur.

Several lines of research arise in light of the results reported here. One is based on the use of nonlinear theory for the behavior of materials undergoing strong displacements; the neo-Hookean material, often used for modeling elastin and collagen, could possibly be used, as well as the *Fung-elastic* constitutive model (Fung 1993, Sun and Sacks 2005), appropriate for soft tissues characterized by pronounced mechanical anisotropy, highly nonlinear stress–strain relationships, large deformations, and viscoelasticity. Another avenue of research consists in developing a model which couples the intravascular and interstitial flow, reducing the need for model constants of uncertain determination. Progress along this line has been recently reported by Wu et al. (2008, 2009). Finally, even assuming that the tumor has a spheroidal shape, given the haphazard formation of cracks, hypoxic and necrotic regions in tissues it is estimated that only about 20% of the cases end up with a spherical distribution of flow and drugs (personal communication of Prof. Fan Yuan), with irregular, three-dimensional infusion in all other cases. This is one of the major problems to overcome when modeling intratumoral infusion.

Conflict of interest statement

The authors declare to have no financial or personal relationships with other people or organizations that could inappropriately influence their work.

Acknowledgements

We gratefully acknowledge the insightful comments by Prof. Fan Yuan, Dr. Rodolfo Repetto and Dr. Marina Artuso.

References

- Barry, S.I., Aldis, G.K., 1990. Comparison of models for flow induced deformation of soft biological tissues. *J. Biomech.* **23**, 647-654
- Baxter, L.T., Jain, R.K., 1989. Transport of fluid and macromolecules in tumors. I. Role of interstitial pressure and convection. *Microvasc. Res.* **37**, 77-104
- Baxter, L.T., Jain, R.K., 1990. Transport of fluid and macromolecules in tumors. II. Role of heterogeneous perfusion and lymphatics. *Microvasc. Res.* **40**, 246-263
- Bonfiglio, A., Leungchavaphongse, K., Repetto, R., Siggers, J. H., 2010. Mathematical modeling of the circulation in the liver lobule. *J. Biomech. Eng (ASME)*, **132**, 111011
- Boucher, Y., J., Kirkwood, M., Opacic, D., Desantis, M., Jain, R.K., 1991. Interstitial hypertension in superficial metastatic melanomas in patients. *Cancer Res.* **51**, 6691–6694
- Fung, Y.C., 1993. *Biomechanics. Mechanical Properties of Living Tissues*. Springer
- Gutmann, R., Leunig, M., Feyh, J., Goetz, A.E., Messmer, K., Kastenbauer, E., Jain, R.K., 1992. Interstitial hypertension in head and neck tumors in patients: Correlation with tumor size. *Cancer Res.* **52**, 1993–1995
- Jain, R.K., 1987. Transport of molecules in the tumor interstitium: a review. *Cancer Res.* **47**, 3039-3051
- Lai, W.M., Mow, V.C., 1980. Drag-induced compression of articular cartilage during a permeation experiment. *Biorheology* **17**, 111-123
- McGuire, S., Yuan, F., 2001. Quantitative analysis of intratumoral infusion of color molecules. *Am. J. Physiol.* **281**, H715-H721
- McGuire, S., Zaharoff, D., Yuan, F., 2006. Nonlinear dependence of hydraulic conductivity on tissue deformation during intratumoral infusion. *Annals Biomed. Eng.* **34**, 1173-1181
- Netti, P.A., Baxter, L.T., Boucher, Y., Skalak, R.K., Jain, R.K., 1995. A poroelastic model for interstitial pressure in tumors. *Biorheology* **32**, 346
- Roh, H. D., Boucher, Y., Kalnicki, S., Buchsbaum, R., Bloomer, W.D., Jain, R.K., 1991. Interstitial hypertension in carcinoma of uterine cervix in patients: Possible correlation with tumor oxygenation and radiation response. *Cancer Res.* **51**, 6695–6698

- Sarntinoranont M., Rooney, F., Ferrari, M., 2003. Interstitial stress and fluid pressure within a growing tumor. *Annals Biomed. Eng.* **31**, 327-335
- Shibley, R.J., and Chapman, S.J., 2010. Multiscale modelling of fluid and drug transport in vascular tumours. *Bull. Math. Biology* **72**, 1464-1491
- Smith, J.H., Humphrey, J.A.C., 2007. Interstitial transport and transvascular fluid exchange during infusion into brain and tumor tissue. *Microvascular Res.* **73**, 58-73
- Sun, W., Sacks, M.S., 2005. Finite element implementation of a generalized Fung-elastic constitutive model for planar soft tissues. *Biomechan. Model Mechanobiol.* **4**, 190–199
- Truskey, G.A., Yuan, F., Katz, D.F., 2009 *Transport phenomena in biological systems*. Pearson Prentice Hall Bioengineering, second edition
- Wu, J., Long, Q., Xu, S., Padhani, A.R., 2009 Study of tumor blood perfusion and its variation due to vascular normalization by anti-angiogenic therapy based on 3D angiogenic microvasculature. *J. Biomech.* **42**, 712-721
- Wu, J., Xu, S., Long, Q., Collins, M.W., König C.S., Zhao, G., Jiang Y., Padhani A.R., 2008. Coupled modeling of blood perfusion in intravascular, interstitial spaces in tumor microvasculature. *J. Biomech.* **41**, 996-1004
- Zhang, X.-Y., Luck, J., Dewhirst, W.M., Yuan, F., 2000. Interstitial hydraulic conductivity in a fibrosarcoma. *Am. J. Physiol.* **279**, H2726-H2734

Figure captions

Fig. 1. Section of a solid tumor of spherical shape. The magnified view on the right shows a detail of the porous interstitium, with the micro-vasculature created around the tumor cells.

Fig. 2. Radial distribution of the hydraulic conductivity coefficient of the capillary walls L_p for cases 1 to 3, as reported in the text.

Fig. 3 Solution of the full model for $\delta = 0.05$. From top left frame, and clockwise: radial distribution of the displacement u , of the hydraulic conductivity K of the tissue, of the flow rate Q through any given spherical surface at radius r (including transvascular fluid exchange), and of the IFP. Cases 1 to 3 with line styles as in fig. 2. The thin horizontal line in the figure with the IFP denotes the dimensionless value of the effective vascular pressure.

Fig. 4 Solution of the full model for $\delta = 0.2$. From top left frame, and clockwise: radial distribution of the displacement u , of the hydraulic conductivity K of the tissue, of the flow rate Q through any given spherical surface at radius r (including transvascular fluid exchange), and of the IFP. Cases 1 to 3 with line styles as in fig. 2. The thin horizontal line in the figure with the IFP denotes the dimensionless value of the effective vascular pressure.

Fig. 5 Inflow rate at $r = a$ as function of the infusion pressure. Symbols are used to denote the experimental data points by McGuire et al. The three cases of fig. 2 are plotted with the same line style used previously. The top curves refer to $K_0 = 3 \times 10^{-5} \text{ cm}^2/(\text{mmHg s})$; the bottom curves, closer to the experimental data, are for $K_0 = 3 \times 10^{-6} \text{ cm}^2/(\text{mmHg s})$. The order zero results of the asymptotic model in the $L_p = L_{p0}$ limit are also displayed, with thin solid lines; when L_p varies (as in fig. 2) the leading order results are but mildly affected.

Fig. 6 Exact (thick solid lines), order zero (this solid lines) and order one asymptotic results (dashed lines) for $p_{\text{infusion}} = 43.75 \text{ mmHg}$ ($\delta = 0.1$) and $K_0 = 3 \times 10^{-6} \text{ cm}^2/(\text{mmHg s})$. The leading order value of u is zero and $K_0 = 1$ (not drawn). The horizontal line in the frame with the IFP denotes the effective vascular pressure.

Fig. 7 Exact (thick solid lines), order zero (this solid lines) and order one asymptotic results (dashed lines) for $p_{\text{infusion}} = 108.75 \text{ mmHg}$ ($\delta = 0.3$) and $K_0 = 3 \times 10^{-6} \text{ cm}^2/(\text{mmHg s})$. The horizontal line in the frame with the IFP denotes the effective vascular pressure.

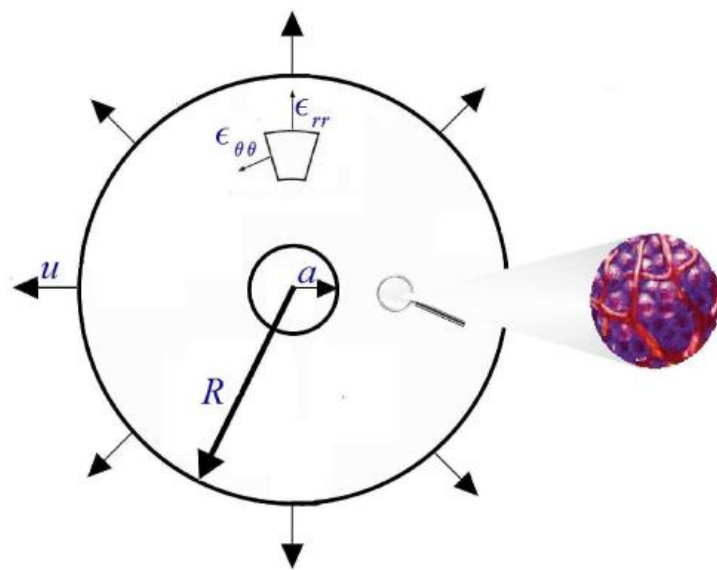


Fig. 1. Section of a solid tumor of spherical shape, with inner cavity filled with fluid. The magnified view on the right shows a detail of the porous interstitium, with the micro-vasculature created around the tumor cells.

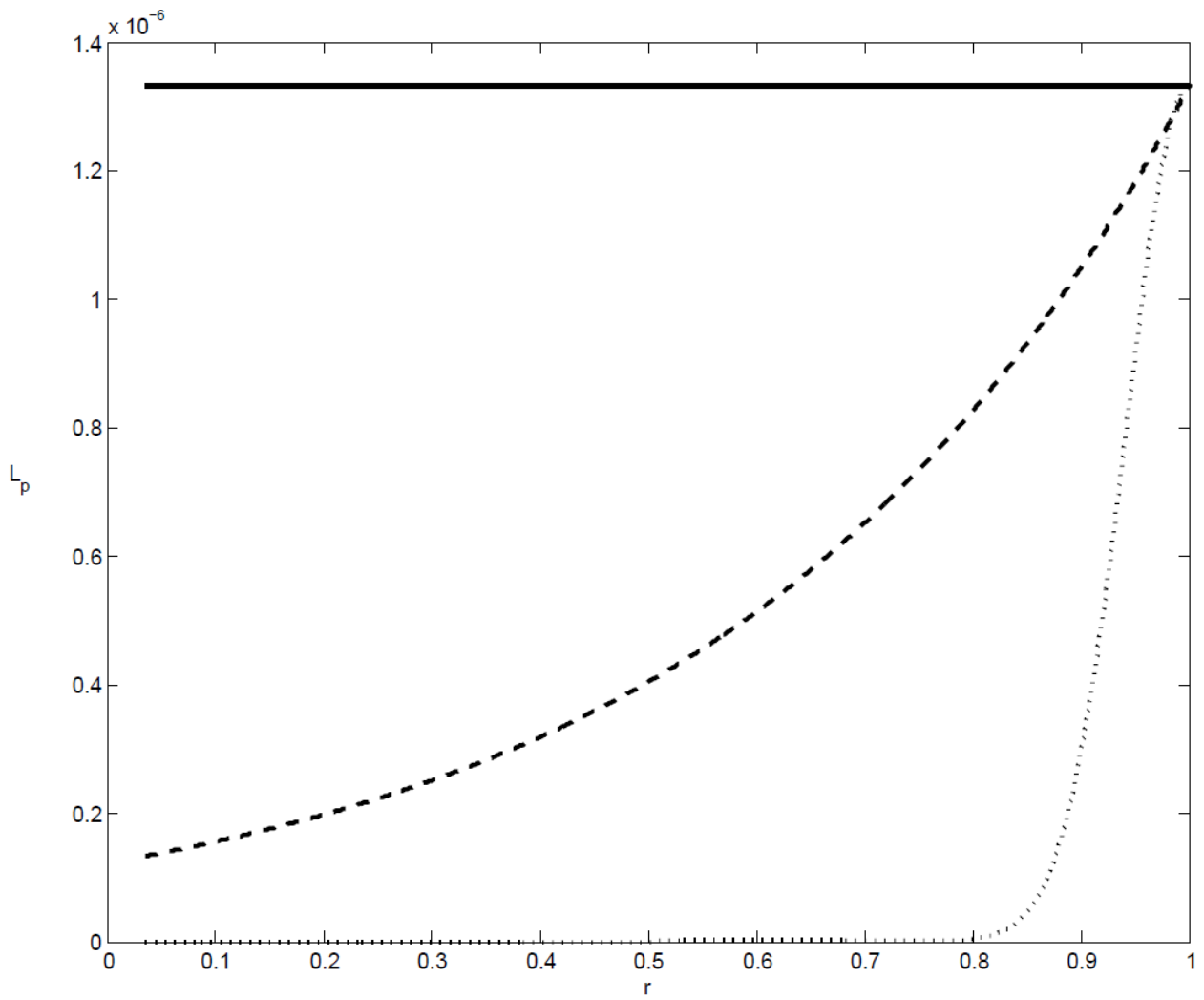


Fig. 2. Radial distribution of the hydraulic conductivity coefficient of the capillary walls L_p for cases 1 to 3, as reported in the text. Case 1: solid line; case 2: dashed line; case 3: dotted line.

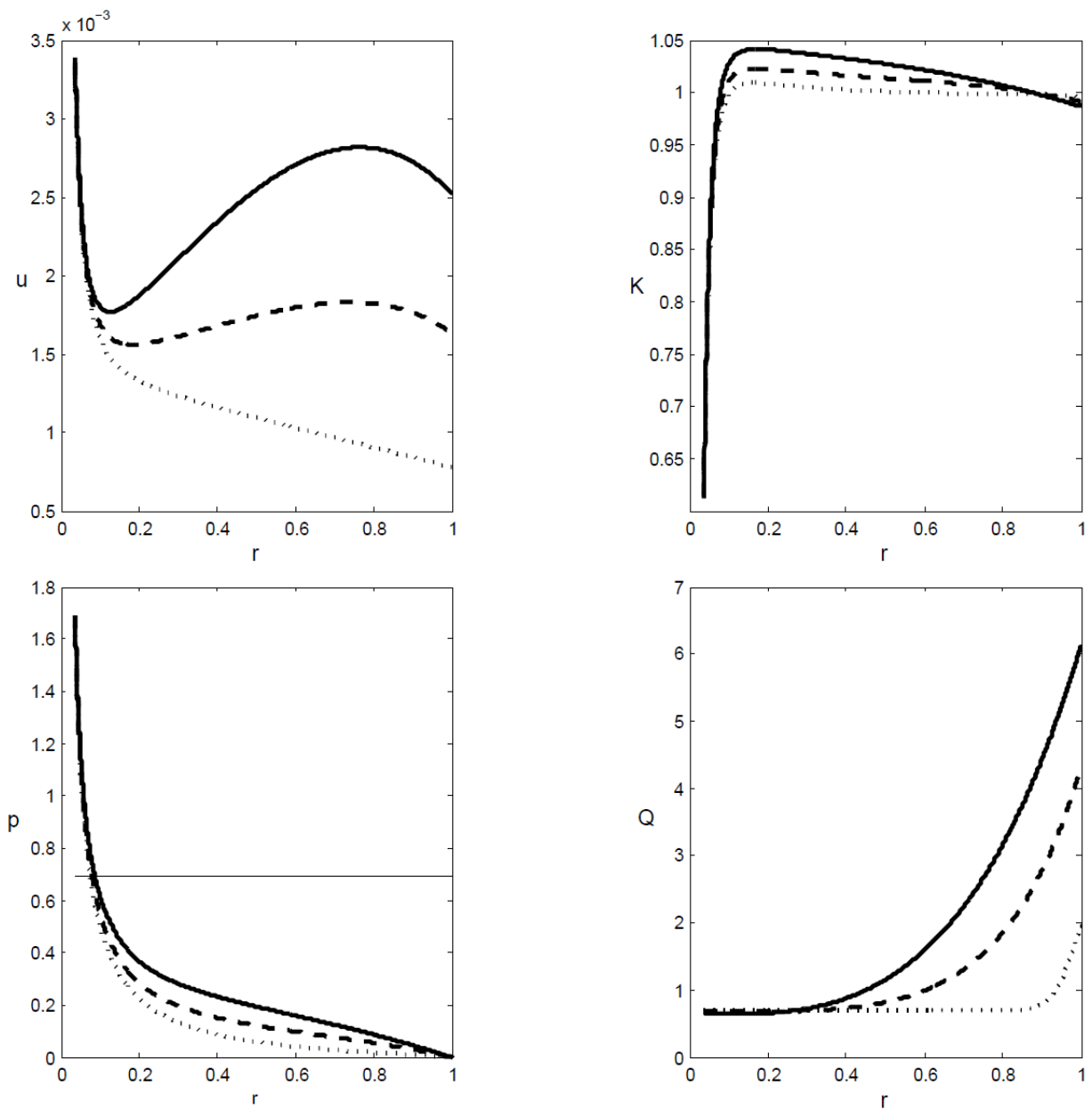


Fig. 3 Solution of the full model for $\delta = 0.05$. From top left frame, and clockwise: radial distribution of the displacement u , of the hydraulic conductivity K of the tissue, of the flow rate Q through any given spherical surface at radius r (including transvascular fluid exchange), and of the IFP. Cases 1 to 3 with line styles as in fig. 2. The thin horizontal line in the figure with the IFP denotes the dimensionless value of the effective vascular pressure.

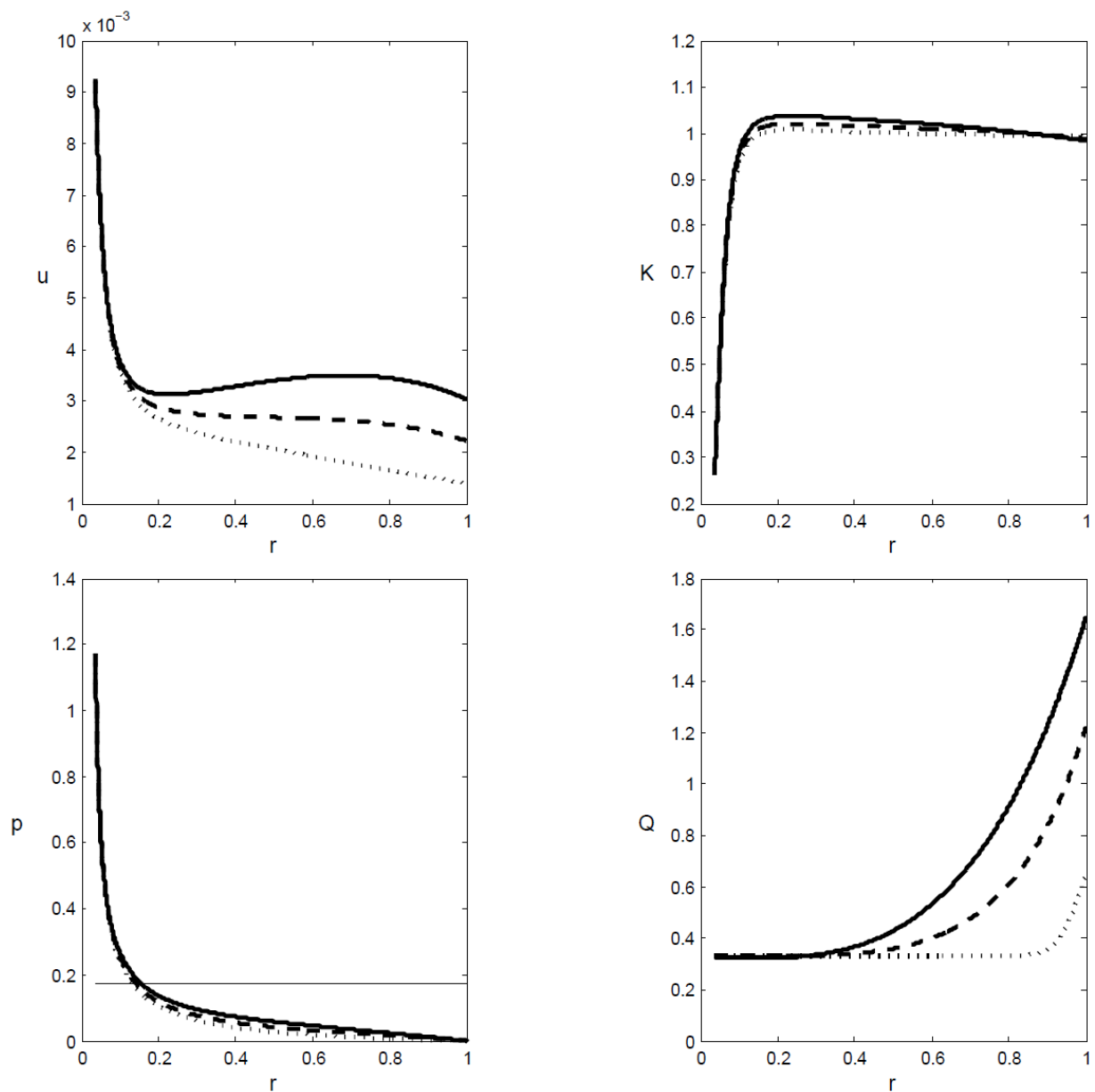


Fig. 4 Solution of the full model for $\delta = 0.2$. From top left frame, and clockwise: radial distribution of the displacement u , of the hydraulic conductivity K of the tissue, of the flow rate Q through any given spherical surface at radius r (including transvascular fluid exchange), and of the IFP. Cases 1 to 3 with line styles as in fig. 2. The thin horizontal line in the figure with the IFP denotes the dimensionless value of the effective vascular pressure.

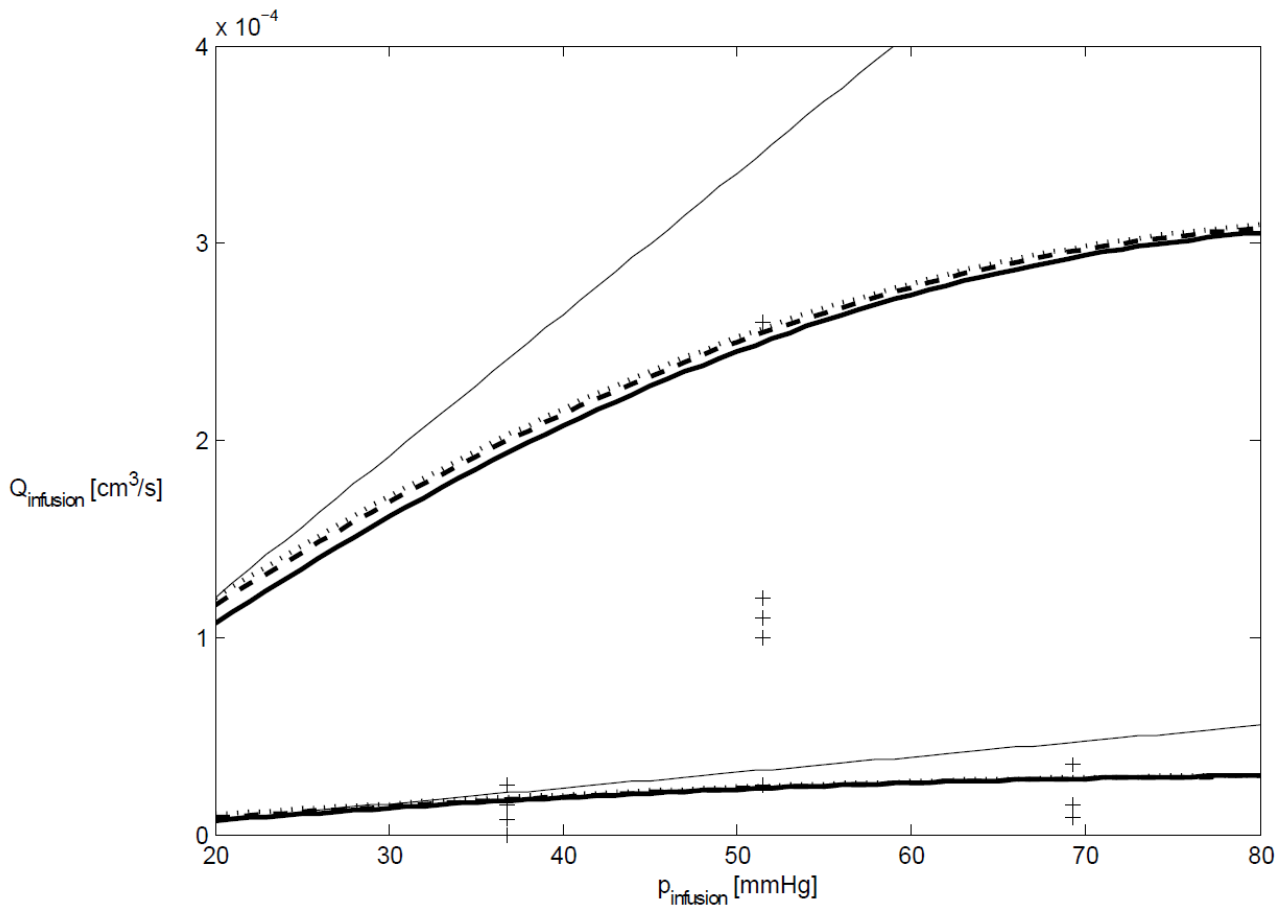


Fig. 5 Inflow rate at $r = a$ as function of the infusion pressure. “Plus” symbols are used to denote the experimental data points by McGuire et al. The three cases of fig. 2 are plotted with the same line style used previously. The top curves refer to $K_0 = 3 \times 10^{-5} \text{ cm}^2/(\text{mmHg s})$; the bottom curves, closer to the experimental data, are for $K_0 = 3 \times 10^{-6} \text{ cm}^2/(\text{mmHg s})$. The order zero results of the asymptotic model in the $L_p = L_{p0}$ limit are also displayed, with thin solid lines; when L_p varies (as in fig. 2) the leading order results are but mildly affected.

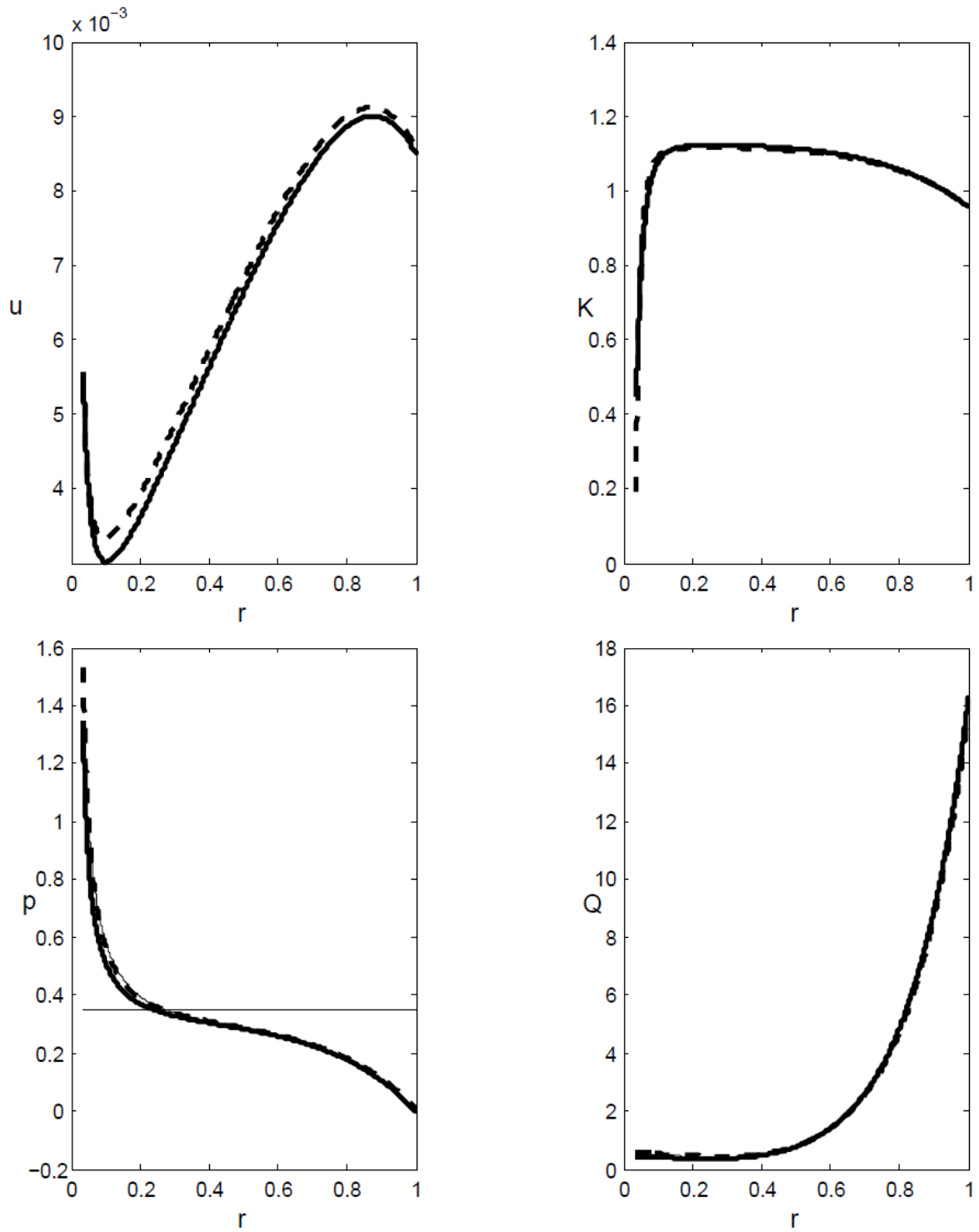


Fig. 6 Exact (thick solid lines), order zero (thin solid lines) and order one asymptotic results (dashed lines) for $p_{\text{infusion}} = 43.75$ mmHg ($\delta = 0.1$) and $K_0 = 3 \times 10^{-6}$ cm²/(mmHg s). The leading order value of u is zero and $K_0 = 1$ (not drawn). The horizontal line in the frame with the IFP denotes the effective vascular pressure.

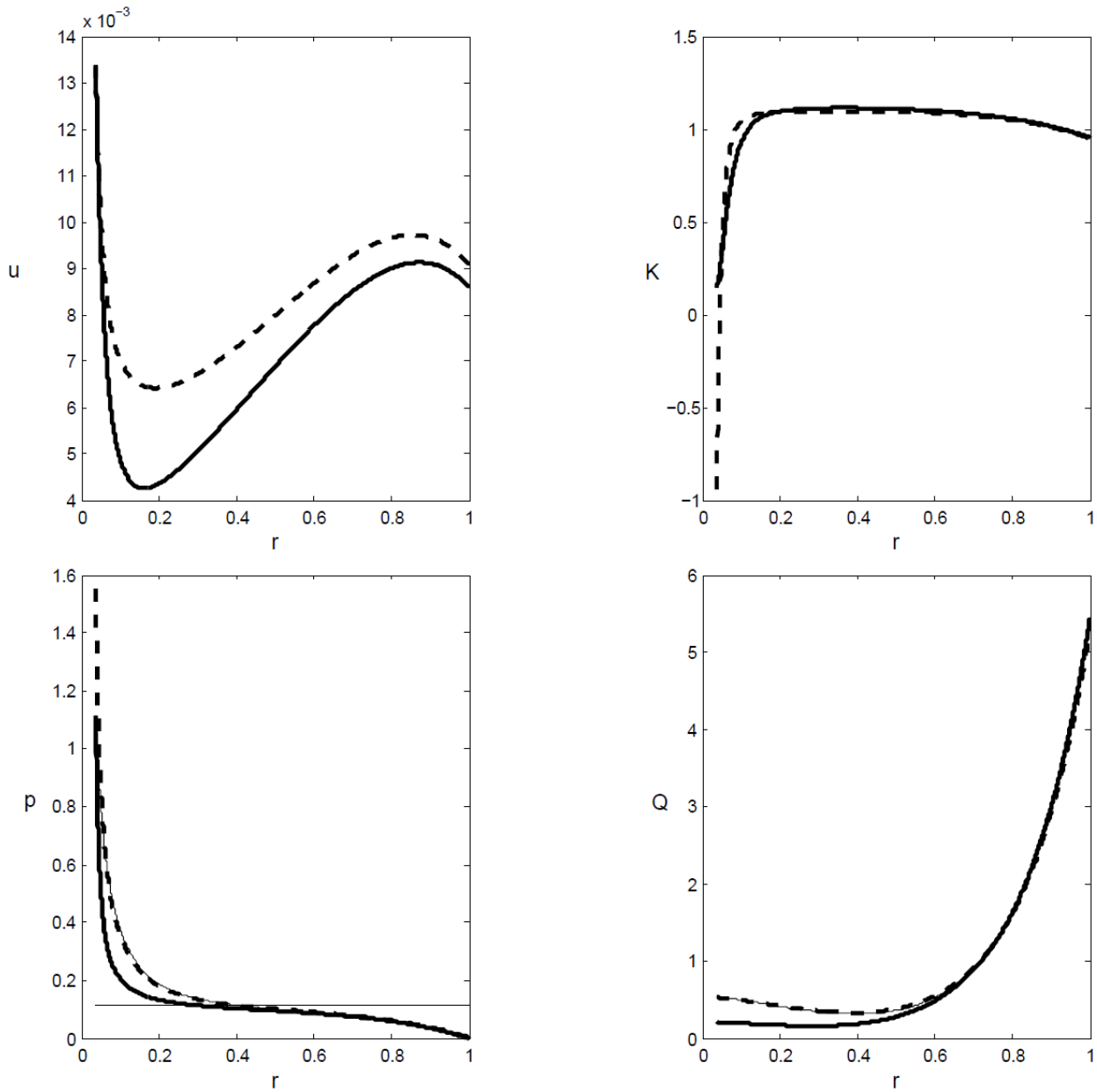


Fig. 7 Exact (thick solid lines), order zero (thin solid lines) and order one asymptotic results (dashed lines) for $p_{\text{infusion}} = 108.75$ mmHg ($\delta = 0.3$) and $K_0 = 3 \times 10^{-6}$ cm²/(mmHg s). The horizontal line in the frame with the IFP denotes the effective vascular pressure.